Supplemental Materials

Molecular Biology of the Cell

Batsios et al.

Supplemental Material

Ate1-mediated post-translational arginylation affects substrate adhesion and cell migration in *Dictyostelium discoideum*

Petros Batsios[a§], Hellen C. Ishikawa-Ankerhold[a¶], Heike Roth[a], Michael Schleicher[a], Catherine C. L. Wong[b], and Annette Müller-Taubenberger[a]*

[a]Department of Cell Biology (Anatomy III), Biomedical Center, LMU Munich, 82152 Planegg-Martinsried, Germany, and [b]National Center for Protein Science Shanghai, Institute of Biochemistry and Cell Biology, Shanghai Institutes of Biological Sciences, Chinese Academy of Sciences, Shanghai 200031, China.

Present address: [§]Cell Biology, Institute for Biochemistry and Biology, University of Potsdam, 14476 Potsdam, Germany; [¶]Department of Cardiology, Walter Brendel Centre of Experimental Medicine, LMU Munich, 81377 Munich, Germany

Figure S1

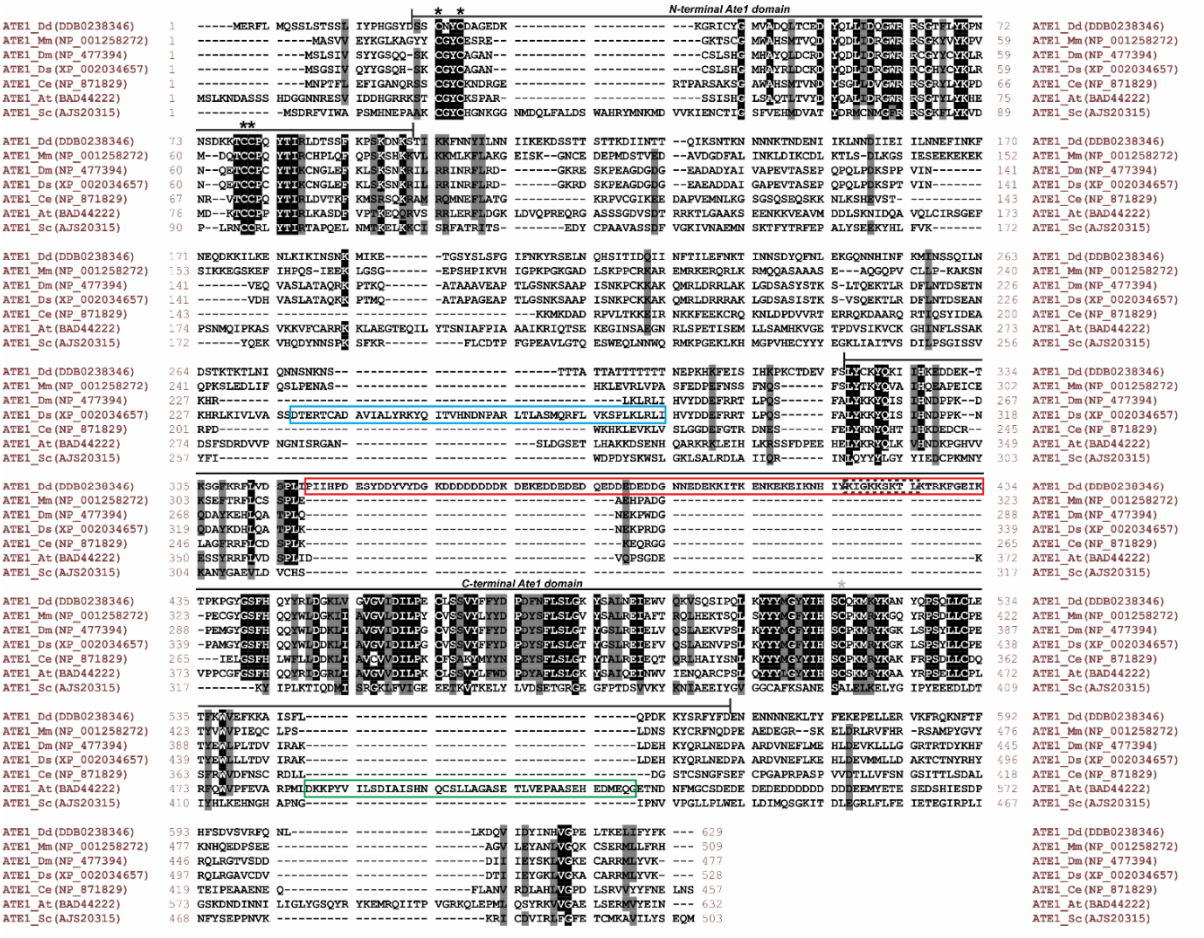

FIGURE S1.**Comparison of Ate1proteins from different organisms.**
Multiple protein sequence alignment of arginyltransferases from *D. discoideum (DDB0238346), M. musculus (NP_001258272), D. melanogaster (NP_477394), D. sechellia (XP_002034657), C. elegans (NP_871829), A. thaliana (BAD44222),* and *S. cerevisiae (AJS20315).* N- and C-terminal Ate1 domains are indicated by black lines. Identicaland similar residues to the Ate1 protein from *Dictyostelium* are labeled in black and gray, respectively. Four conserved cysteine residues (black stars) were shown to be important for the enzymatic activity of *S. cerevisiae* Ate1p (Li and Pickart, 1995), and one cysteine (gray star) is conserved in Ate proteins, but is not required for the enzymatic activity. The interrupted domain architecture of Ate1 in *D. sechellia*,*D. discoideum* and *A. thaliana* with amino acid insertions at various positions of the C-terminus are indicated with cyan, red and green boxes, respectively. In the sequence of *D. discoideum*, a basic consensus sequence similar to common nuclear localization signals is shown by the doted box as predicted by ELM and with NLS mapper (http://nls-mapper.iab.keio.ac.jp).

Figure S2

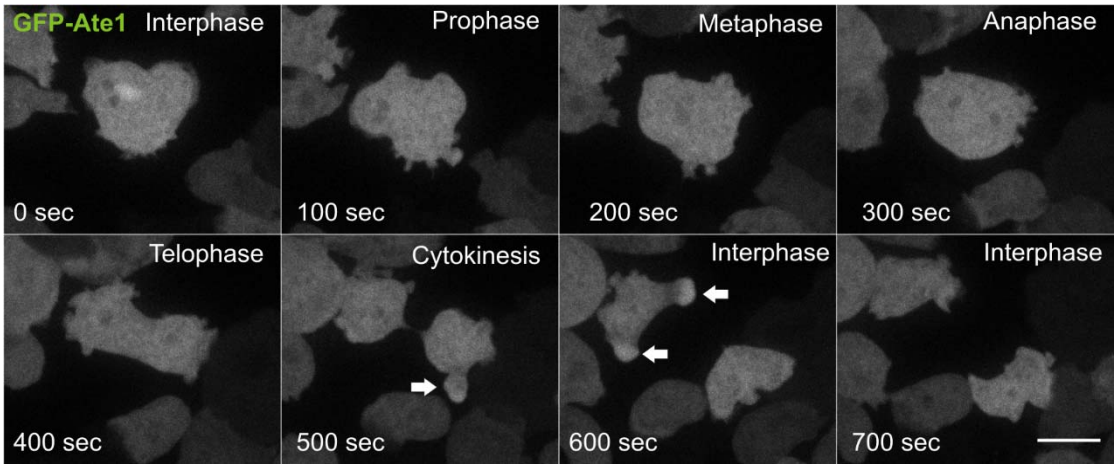

FIGURE S2. **Subcellular localization ofDdAte1-GFP during cell division.**
A *Dictyostelium* cell expressing DdAte1-GFP was recorded during cell division by spinning disk confocal microscopy. The fluorescence signal of DdAte1-GFP enriched in the nucleus disappears with the onset of mitosis. After completion of cytokinesis, the DdAte1-GFPsignal reappears at newly formed pseudopodia (arrows). Please compare to Supplemental Movie2.Scale Bar, 5 μm.

Figure S3

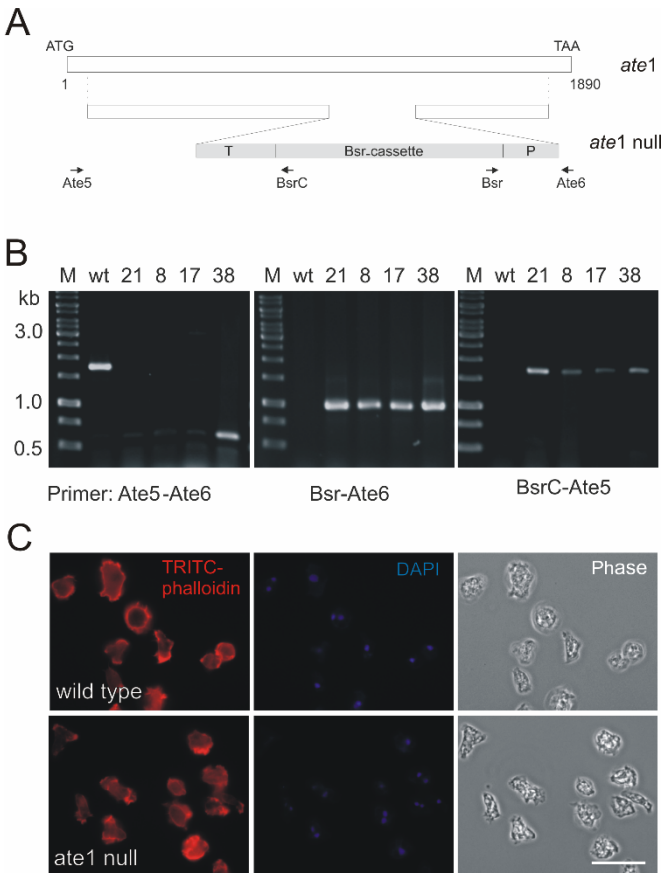

FIGURE S3. ***Ate1* gene disruption.**
(A) Scheme of the *ate1* knockout construct. Bsr (blasticidin resistance) cassette flanked by a 5′-UTR and a 3′-UTR of *ate1* can displace the endogenous *ate1* gene. Black arrows indicate the oligonucleotides used to test for a knockout event. (B) By PCR, four independent *ate1*-minus clones were identified (clone numbers 21, 8, 17, and 38). Wild type (wt) genomic DNA was used as control. (C) *Ate1*-null cells stained with TRITC-phalloidin showed no significant differences in the localization of F-actin in comparison to wild-type cells, but*ate1*-null cells were smaller than wild-type cells. Scale Bar, 10 µm.

Figure S4

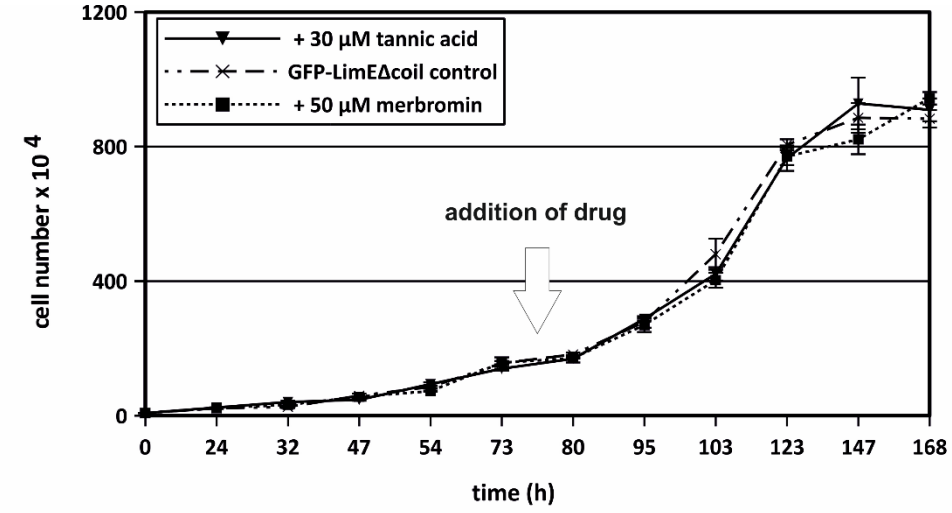

FIGURE S4**. Merbromin and tannic acid do not affect cell growth.**
GFP-LimEΔcoil expressing wild-type cells were grown in shaking cultures. Either 50 µM merbromin or 30 µM tannic acid were added at the indicated time point (arrow), and growth was compared to untreated control cells.

SUPPLEMENTALTABLES

TABLE S1. **DTASelect file of validated peptides.**
DTASelect filtering was performed using DTASelect v2.1.3 followed by manual data validation as described (Wong et al., 2007, Xu et al., 2009). Manually validated peptides of actin isoforms (Table 1) are highlighted in yellow.

TABLE S2. **Chromatogram data of validated peptides.**
Scan numbers and MS1 precursors with intensity and time information are shown. The corresponding ms2 file and additional information is available upon request from the authors.

MOVIE LEGENDS

MOVIE 1. Representative FRAP experiment at a protrusion ofa *Dictyostelium* cell expressing Ate1-GFP.The photo-bleaching event is stamped into the movie at 20 s. Scale bar, 5 μm.

MOVIE 2. Spinning disk confocal imaging of a *Dictyostelium* cell expressing Ate1-GFP during cell division.

MOVIE 3. RICM of a *Dictyostelium* wild-type cell. Dark areas indicate close contact to the substrate surface. Note the constant spreading and de-attachment to the substratum.Left: phase contrast, right: RICM. Bar, 5 μm.

MOVIE 4. RICM of a *Dictyostelium ate1*-null cell. Dark areas indicate a close contact to the substrate surface. *Ate1*-null cells never spread on the substratum as closely as do wild-type cells. Left: phase contrast, right: RICM. Bar, 5 μm.

MOVIE 5. RICM of a *Dictyostelium* Ate1-rescued cell*(ate1*-null cell expressing Ate1-GFP). Dark areas indicate close contact to the substrate surface. Note the constant spreading and de-attachment to the substratum as observed in wild type (Movie 3). Left: phase contrast, right: RICM. Bar, 10 μm.

MOVIE 6.Actin network dynamics visualized by expression of LimEΔcoil-GFP in *Dictyosteliumdiscoideum* wild-type cells. Recording was by confocal microscopy. The focal plane was moved in z-axis towards the substrate adhesion site. Scale bar, 10 μm.

MOVIE 7. Actin network dynamics visualized by expression of LimEΔcoil-GFP in *Dictyosteliumdiscoideum ate1*-null cells (clone #1-21). Recording was by confocal microscopy. The focal plane was moved in z-direction. Scale bar, 10 μm.

MOVIE 8. Actin network dynamics visualized by expression of LimEΔcoil-GFP in *Dictyosteliumdiscoideum ate1*-null cells (clone #2-17). Recording was by confocal microscopy. The focal plane was moved in z-direction. Scale bar, 10 μm.

MOVIE 9. Actin network dynamics visualized by expression of LimEΔcoil-GFP in *Dictyosteliumdiscoideum* wild-type (left) and *ate1*-null (right) cells. Recording was by TIRF microscopy. The focal plane was moved in z-direction. Scale bar, 5 μm.

MOVIE 10. Chemotaxis of *ate1*-null cells expressing GFP-LimEΔcoil (green), and wild-type cells expressing RFP-LimEΔcoil (red). Fluorescently labeled LimEΔcoil visualizes filamentous actin, and was employed here to distinguish wild-type and *ate1*-null cells. Aggregation-competent cells were exposed to chemoattractant gradients by moving a micropipette filled with cAMP. Cells were recorded by confocal microscopy. Note that mutant cells (green) migrate faster than wild type (red). Scale bar, 20 μm.

Scan number and mz precursor mass 028896 975.93427
010980 59.11 975.89117 54942.5
010981 59.11 975.89117 54942.5
018898 96.93 975.92865 302886.9
018899 96.94 975.92865 302886.9
019711 100.62 975.92438 3179749.3
019712 100.62 975.92438 3179749.3
021783 111.08 975.93048 35515.9
021784 111.09 975.93048 35515.9
028896 146.33 975.93427 63463.1
028897 146.33 975.93427 63463.1
031101 157.21 975.93756 95326.8
031102 157.21 975.93756 95326.8
031309 158.3 975.9386 93144.4
031310 158.3 975.9386 93144.4
031989 161.75 975.93567 123545.4
031990 161.75 975.93567 123545.4
033291 168.15 975.93805 152645.9
033292 168.15 975.93805 152645.9
039708 200.08 975.94446 23240.0
039709 200.08 975.94446 23240.0
Scan number and mz precursor mass 016957 774.87421
010980 59.11 975.89117 54942.5
010981 59.11 975.89117 54942.5
018898 96.93 975.92865 302886.9
018899 96.94 975.92865 302886.9
019711 100.62 975.92438 3179749.3
019712 100.62 975.92438 3179749.3
021783 111.08 975.93048 35515.9
021784 111.09 975.93048 35515.9
028896 146.33 975.93427 63463.1
028897 146.33 975.93427 63463.1
031101 157.21 975.93756 95326.8
031102 157.21 975.93756 95326.8
031309 158.3 975.9386 93144.4
031310 158.3 975.9386 93144.4
031989 161.75 975.93567 123545.4
031990 161.75 975.93567 123545.4
033291 168.15 975.93805 152645.9
033292 168.15 975.93805 152645.9
039708 200.08 975.94446 23240.0
039709 200.08 975.94446 23240.0
Scan number and mz precursor mass 013232 613.77692
010980 59.11 975.89117 54942.5
010981 59.11 975.89117 54942.5
018898 96.93 975.92865 302886.9
018899 96.94 975.92865 302886.9
019711 100.62 975.92438 3179749.3
019712 100.62 975.92438 3179749.3
021783 111.08 975.93048 35515.9
021784 111.09 975.93048 35515.9
028896 146.33 975.93427 63463.1
028897 146.33 975.93427 63463.1
031101 157.21 975.93756 95326.8
031102 157.21 975.93756 95326.8
031309 158.3 975.9386 93144.4
031310 158.3 975.9386 93144.4
031989 161.75 975.93567 123545.4
031990 161.75 975.93567 123545.4
033291 168.15 975.93805 152645.9
033292 168.15 975.93805 152645.9
039708 200.08 975.94446 23240.0

039709 200.08 975.94446 23240.0
Scan number and mz precursor mass 018772 992.04828
010980 59.11 975.89117 54942.5
010981 59.11 975.89117 54942.5
018898 96.93 975.92865 302886.9
018899 96.94 975.92865 302886.9
019711 100.62 975.92438 3179749.3
019712 100.62 975.92438 3179749.3
021783 111.08 975.93048 35515.9
021784 111.09 975.93048 35515.9
028896 146.33 975.93427 63463.1
028897 146.33 975.93427 63463.1
031101 157.21 975.93756 95326.8
031102 157.21 975.93756 95326.8
031309 158.3 975.9386 93144.4
031310 158.3 975.9386 93144.4
031989 161.75 975.93567 123545.4
031990 161.75 975.93567 123545.4
033291 168.15 975.93805 152645.9
033292 168.15 975.93805 152645.9
039708 200.08 975.94446 23240.0
039709 200.08 975.94446 23240.0
Scan number and mz precursor mass 029129 1006.54816
010980 59.11 975.89117 54942.5
010981 59.11 975.89117 54942.5
018898 96.93 975.92865 302886.9
018899 96.94 975.92865 302886.9
019711 100.62 975.92438 3179749.3
019712 100.62 975.92438 3179749.3
021783 111.08 975.93048 35515.9
021784 111.09 975.93048 35515.9
028896 146.33 975.93427 63463.1
028897 146.33 975.93427 63463.1
031101 157.21 975.93756 95326.8
031102 157.21 975.93756 95326.8
031309 158.3 975.9386 93144.4
031310 158.3 975.9386 93144.4
031989 161.75 975.93567 123545.4
031990 161.75 975.93567 123545.4
033291 168.15 975.93805 152645.9
033292 168.15 975.93805 152645.9
039708 200.08 975.94446 23240.0
039709 200.08 975.94446 23240.0
Scan number and mz precursor mass 031933 1092.54846
010980 59.11 975.89117 54942.5
010981 59.11 975.89117 54942.5
018898 96.93 975.92865 302886.9
018899 96.94 975.92865 302886.9
019711 100.62 975.92438 3179749.3
019712 100.62 975.92438 3179749.3
021783 111.08 975.93048 35515.9
021784 111.09 975.93048 35515.9
028896 146.33 975.93427 63463.1
028897 146.33 975.93427 63463.1
031101 157.21 975.93756 95326.8
031102 157.21 975.93756 95326.8
031309 158.3 975.9386 93144.4
031310 158.3 975.9386 93144.4
031989 161.75 975.93567 123545.4
031990 161.75 975.93567 123545.4
033291 168.15 975.93805 152645.9
033292 168.15 975.93805 152645.9

039708 200.08 975.94446 23240.0
039709 200.08 975.94446 23240.0
Scan number and mz precursor mass 017132 671.36395
010980 59.11 975.89117 54942.5
010981 59.11 975.89117 54942.5
018898 96.93 975.92865 302886.9
018899 96.94 975.92865 302886.9
019711 100.62 975.92438 3179749.3
019712 100.62 975.92438 3179749.3
021783 111.08 975.93048 35515.9
021784 111.09 975.93048 35515.9
028896 146.33 975.93427 63463.1
028897 146.33 975.93427 63463.1
031101 157.21 975.93756 95326.8
031102 157.21 975.93756 95326.8
031309 158.3 975.9386 93144.4
031310 158.3 975.9386 93144.4
031989 161.75 975.93567 123545.4
031990 161.75 975.93567 123545.4
033291 168.15 975.93805 152645.9
033292 168.15 975.93805 152645.9
039708 200.08 975.94446 23240.0
039709 200.08 975.94446 23240.0
Scan number and mz precursor mass 034957 1076.21533
010980 59.11 975.89117 54942.5
010981 59.11 975.89117 54942.5
018898 96.93 975.92865 302886.9
018899 96.94 975.92865 302886.9
019711 100.62 975.92438 3179749.3
019712 100.62 975.92438 3179749.3
021783 111.08 975.93048 35515.9
021784 111.09 975.93048 35515.9
028896 146.33 975.93427 63463.1
028897 146.33 975.93427 63463.1
031101 157.21 975.93756 95326.8
031102 157.21 975.93756 95326.8
031309 158.3 975.9386 93144.4
031310 158.3 975.9386 93144.4
031989 161.75 975.93567 123545.4
031990 161.75 975.93567 123545.4
033291 168.15 975.93805 152645.9
033292 168.15 975.93805 152645.9
039708 200.08 975.94446 23240.0
039709 200.08 975.94446 23240.0
Scan number and mz precursor mass 028047 719.34888
010980 59.11 975.89117 54942.5
010981 59.11 975.89117 54942.5
018898 96.93 975.92865 302886.9
018899 96.94 975.92865 302886.9
019711 100.62 975.92438 3179749.3
019712 100.62 975.92438 3179749.3
021783 111.08 975.93048 35515.9
021784 111.09 975.93048 35515.9
028896 146.33 975.93427 63463.1
028897 146.33 975.93427 63463.1
031101 157.21 975.93756 95326.8
031102 157.21 975.93756 95326.8
031309 158.3 975.9386 93144.4
031310 158.3 975.9386 93144.4
031989 161.75 975.93567 123545.4
031990 161.75 975.93567 123545.4
033291 168.15 975.93805 152645.9

033292 168.15 975.93805 152645.9
039708 200.08 975.94446 23240.0
039709 200.08 975.94446 23240.0
Scan number and mz precursor mass 025505 597.63489
010980 59.11 975.89117 54942.5
010981 59.11 975.89117 54942.5
018898 96.93 975.92865 302886.9
018899 96.94 975.92865 302886.9
019711 100.62 975.92438 3179749.3
019712 100.62 975.92438 3179749.3
021783 111.08 975.93048 35515.9
021784 111.09 975.93048 35515.9
028896 146.33 975.93427 63463.1
028897 146.33 975.93427 63463.1
031101 157.21 975.93756 95326.8
031102 157.21 975.93756 95326.8
031309 158.3 975.9386 93144.4
031310 158.3 975.9386 93144.4
031989 161.75 975.93567 123545.4
031990 161.75 975.93567 123545.4
033291 168.15 975.93805 152645.9
033292 168.15 975.93805 152645.9
039708 200.08 975.94446 23240.0
039709 200.08 975.94446 23240.0
Scan number and mz precursor mass 038278 846.83563
010980 59.11 975.89117 54942.5
010981 59.11 975.89117 54942.5
018898 96.93 975.92865 302886.9
018899 96.94 975.92865 302886.9
019711 100.62 975.92438 3179749.3
019712 100.62 975.92438 3179749.3
021783 111.08 975.93048 35515.9
021784 111.09 975.93048 35515.9
028896 146.33 975.93427 63463.1
028897 146.33 975.93427 63463.1
031101 157.21 975.93756 95326.8
031102 157.21 975.93756 95326.8
031309 158.3 975.9386 93144.4
031310 158.3 975.9386 93144.4
031989 161.75 975.93567 123545.4
031990 161.75 975.93567 123545.4
033291 168.15 975.93805 152645.9
033292 168.15 975.93805 152645.9
039708 200.08 975.94446 23240.0
039709 200.08 975.94446 23240.0
Scan number and mz precursor mass 038957 846.83392
010980 59.11 975.89117 54942.5
010981 59.11 975.89117 54942.5
018898 96.93 975.92865 302886.9
018899 96.94 975.92865 302886.9
019711 100.62 975.92438 3179749.3
019712 100.62 975.92438 3179749.3
021783 111.08 975.93048 35515.9
021784 111.09 975.93048 35515.9
028896 146.33 975.93427 63463.1
028897 146.33 975.93427 63463.1
031101 157.21 975.93756 95326.8
031102 157.21 975.93756 95326.8
031309 158.3 975.9386 93144.4
031310 158.3 975.9386 93144.4
031989 161.75 975.93567 123545.4
031990 161.75 975.93567 123545.4

033291	168.15	975.93805	152645.9
033292	168.15	975.93805	152645.9
039708	200.08	975.94446	23240.0
039709	200.08	975.94446	23240.0